AD-453913

DISCLAIMER NOTICE

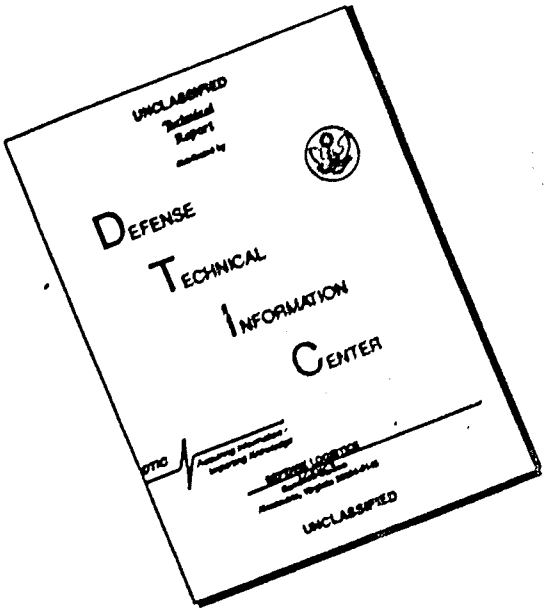

THIS DOCUMENT IS BEST QUALITY AVAILABLE. THE COPY FURNISHED TO DTIC CONTAINED A SIGNIFICANT NUMBER OF PAGES WHICH DO NOT REPRODUCE LEGIBLY.

BRL

MEMORANDUM REPORT
NO. 1606

ATTENUATION OF PLANE SHOCK FRONTS IN ALUMINUM

By F. E. Allison

NOVEMBER 1964

U. S. ARMY MATERIEL COMMAND
BALLISTIC RESEARCH LABORATORIES
ABERDEEN PROVING GROUND, MARYLAND

Destroy this report when it is no longer needed.
Do not return it to the originator.

B A L L I S T I C R E S E A R C H L A B O R A T O R I E S

MEMORANDUM REPORT NO. 1606

NOVEMBER 1964

ATTENUATION OF PLANE SHOCK FRONTS IN ALUMINUM*

F. E. Allison

Terminal Ballistics Laboratory

*This work was partially supported by ARPA funds.

RDT & E Project No. 1M010501A009

A B E R D E E N P R O V I N G G R O U N D, M A R Y L A N D

B A L L I S T I C R E S E A R C H L A B O R A T O R I E S

MEMORANDUM REPORT NO. 1606

FEAllison/mb
Aberdeen Proving Ground, Md.
November 1964

ATTENUATION OF PLANE SHOCK FRONTS IN ALUMINUM

ABSTRACT

The attenuation of a plane shock wave by an overtaking rarefaction has been studied using a rotating-mirror streak camera to obtain a shock trajectory resulting from the impact of a thin striker. Experimental data are presented for shocks in 1100F aluminum and the data are compared with results obtained from two sets of calculations. The shock attenuation is in excellent agreement with calculations based on linear characteristics along which (u + c) is constant. The attenuation is measurably less than that calculated from Fowles' equations, which neglect entropy changes at the shock front.

TABLE OF CONTENTS

	Page
ABSTRACT	3
TABLE OF SYMBOLS	7
INTRODUCTION	9
METHODS USED TO CALCULATE SHOCK TRAJECTORIES	10
EXPERIMENTAL OBSERVATIONS	15
DISCUSSION OF RESULTS	19
ACKNOWLEDGEMENTS	19
REFERENCES	21
DISTRIBUTION LIST	23

TABLE OF SYMBOLS

c	sound velocity (c^2 = bulk modulus/density), mm/μsec
c_o	sound velocity of the undisturbed media, mm/μsec
c_1	sound velocity immediately behind the shock front, mm/μsec
d	striker plate thickness, mm
p	pressure, kilobars
t	time, μsec
t_1	time required for the shock to reach the rear surface of the striker, μsec
t_2	time required for the shock to reach the rear surface of the striker and the lead C^+ characteristic to reach the striker-target interface, μsec
t_3	time required for the shock to reach the rear surface of the striker and the lead C^+ characteristic to overtake the shock in the target, μsec
u	particle velocity at the shock front, mm/μsec
u_1	particle velocity immediately after impact, mm/μsec
x	space coordinate, mm
x_1	position of the rear surface of the striker when the shock front arrives at the surface, mm
x_2	position of the striker-target interface when the lead C^+ characteristic reaches the interface, mm
x_3	position of the shock front in the target when the lead C^+ characteristic overtakes the shock, mm
z	$(u + c)$, mm/μsec
z_1	$(u_1 + c_1)$, mm/μsec
A	constant in the Murnaghan equation, kilobars (188.96 kilobars for aluminum)
U	shock velocity, mm/μsec

TABLE OF SYMBOLS

U_o	initial value of shock velocity in the target, mm/sec
U'_o	initial value of shock velocity in the striker, mm/μsec
V	impact velocity, mm/μsec
γ	constant in the Murnaghan equation, dimensionless (4.266 for aluminum)
ρ	density, gm/cm^3
ρ_o	density ahead of the shock front, gm/cm^3
σ	dimensionless parameter equal to $(u + c - c_o)/c_o$

Note: The quantities t_2 and x_2 are not used in the discussions presented in this report. They are included here in order to make the remainder of the symbols agree with those used by Chou and Fowles.

INTRODUCTION

The impact of a thin striker plate on a thick target of the same material produces two plane shock waves, one propagating back into the striker and the other propagating forward into the target. The initial strengths of the two shocks are equal and uniquely determined by the impact velocity and the Hugoniot properties of the material. When the shock in the striker reaches the rear surface of the plate a centered rarefaction is propagated forward, eventually overtakes the forward moving shock, and reduces its velocity. Attenuation of plane shock waves in solids has been treated by G. R. Fowles[1*] in 1960 and more recently by Chou, Sidhu, and Zajac[2]. Fowles assumes that the change in entropy across the shock can be neglected, an approximation valid in the limit of weak shocks. Chou and his collaborators have obtained detailed graphical solutions of the characteristic equations and have compared these solutions with analytical solutions based on the assumption that the C^+ characteristics are linear. For aluminum, the approximate analytical solutions are in good agreement with the detailed graphical solutions. The assumption of linear characteristics was used somewhat earlier by Al'tshuler et al[3] to calculate from experimental data the sound velocity behind a strong shock. Although details are not given in their paper, they also performed numerical calculations to show that the error resulting from the use of straight characteristic lines is small.

The work described in this report was undertaken in an effort to provide an experimental evaluation of the theoretical approximations described in the preceding paragraphs. Distance-time trajectories for shocks propagating into soft aluminum targets were precisely determined by optical methods. The experimental results are compared with two sets of calculations: one based on the approximations of Chou et al and the other based on the approximations of Fowles.

---

* Superscript numbers denote references found on page 21.

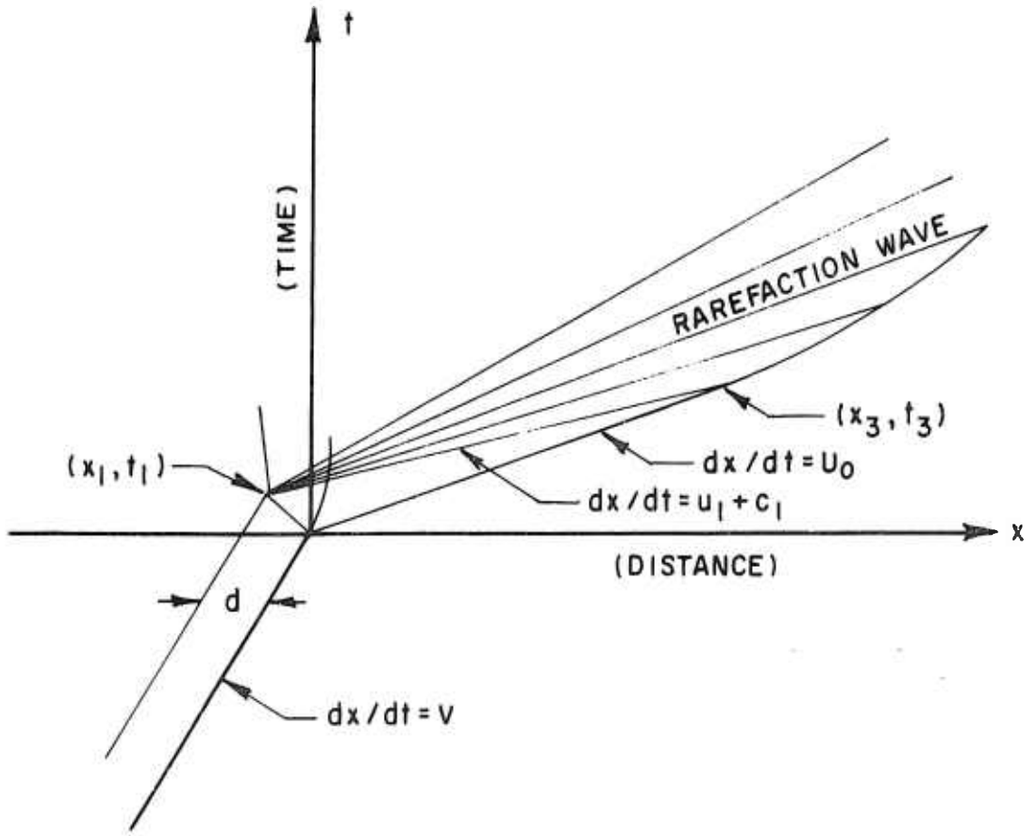

FIGURE I- DIAGRAM ILLUSTRATING THE ATTENUATION OF A PLANE SHOCK WAVE BY AN OVERTAKING RAREFACTION ORGINATING FROM THE REAR SURFACE OF THE STRIKER.

METHODS USED TO CALCULATE SHOCK TRAJECTORIES

Chou's Approximation for (u + c) Constant.

Figure 1 illustrates the shock attenuation problem in the physical (x, t) plane. Impact between the front surface of the striker and the rear surface of the target occurs at x = 0, t = 0. The Rankine-Hugoniot relations for mass and momentum conservation together with the continuity of pressure and particle velocity at the interface can be used to show that

$$u_1 = \frac{V}{2} \quad , \tag{1}$$

and

$$U_o' = -(U_o - V) \quad , \tag{2}$$

where u_1 is the particle velocity; V, the impact velocity; U_o', the shock velocity in the striker; and U_o, the shock velocity in the target. All velocities are measured relative to a stationary observer.

From an inspection of Figure 1, we note that

$$x_1 = -t_1 (U_o - V) \quad , \tag{3}$$

$$x_1 = -d + V t_1 \quad . \tag{4}$$

When Equations (3) and (4) are solved for x_1 and t_1, we obtain

$$x_1 = -d (1 - V/U_o) \quad , \tag{5}$$

$$t_1 = d/U_o \quad . \tag{6}$$

The intersection of the leading C^+ characteristics with the shock trajectory occurs at the point (x_3, t_3). As illustrated in Figure 1

$$x_3 = U_o t_3 \quad , \tag{7}$$

$$(x_3 - x_1) = (u_1 + c_1)(t_3 - t_1) \quad , \tag{8}$$

where u_1 and c_1 are the particle and sound velocities along the lead characteristics. When Equations (7) and (8) are solved for x_3 and t_3 we obtain

$$x_3 = d\left[2(U_o + c_1) - V\right]/\left[V - 2(U_o - c_1)\right] \tag{9}$$

$$t_3 = x_3/U_o \tag{10}$$

after eliminating u_1 and x_1 by means of Equations (1) and (5).

If all C^+ characteristics are assumed to be linear, then the intersection of other characteristics with the shock trajectory is given by

$$x - x_1 = z(t - t_1) \quad , \tag{11}$$

$$x = x_3 + \int_{t_3}^{t} U \, dt \quad , \tag{12}$$

where $z = (u + c)$ is a constant along each characteristic.
For any given value of the parameter z Equations (11) and (12) represent two equations involving the variables x and t. If both equations are differentiated with respect to t and dx/dt eliminated between the two, one obtains

$$U = z + (t - t_1)\frac{dz}{dt} \quad , \tag{13}$$

which can be integrated to give

$$t = t_1 + (t_3 - t_1) \exp \int_{z_1}^{z} \frac{dz}{U-z} \quad . \tag{14}$$

When t , obtained from Equation (14), is substituted into Equation (11) one obtains

$$x = x_1 + z\,(t_3 - t_1) \exp \int_{z_1}^{z} \frac{dz}{U-z} \quad . \tag{15}$$

Equations (14) and (15) are parametric equations for the shock trajectory in which x and t are expressed as functions of the parameter z.

Fowles' Approximation.

In his analysis Fowles fits the experimental Hugoniot with a semi-theoretical relation derived by Murnaghan[4], which relates the pressure and density by an equation of the form

$$p = A\left[(\rho/\rho_o)^{\gamma} - 1\right] \quad . \tag{16}$$

Fowles used the Los Alamos shock wave data[5] to evaluate the constants A and γ. For aluminum he obtained 188.96 kilobars for A and 4.266 for γ. Since entropy changes across the shock are neglected, the Hugoniot and adiabat are identical; hence,

$$c^2 = \frac{A\gamma}{\rho_o}\left(\frac{\rho}{\rho_o}\right)^{\gamma-1} = c_o^{\,2}\left(\frac{\rho}{\rho_o}\right)^{\gamma-1} \quad . \tag{17}$$

As shown in Table I, Equation (16) represents the pressure data to within 1 percent over the entire pressure range from a hundred kilobars to one megabar. However, the sound velocities are larger than the Los Alamos results by about 3.5 percent at a hundred kilobars and by about 14.5 percent at one megabar.

By combining Equation (16) with Equation (1) and making use of the Rankine-Hugoniot jump conditions, the density behind the shock front can be related to the impact velocity.
The resulting expression,

$$(V/2)^2 = (A/\rho_o)(1 - \rho_o/\rho_1)\left[(\rho_1/\rho_o)^{\gamma} - 1\right] \quad , \tag{18}$$

is most easily solved by graphical or numerical methods. For t and x, Fowles obtains the relations

$$t(\sigma) = t_1 + (t_3 - t_1)\left[\frac{\sigma_o}{\sigma_o - 2(\gamma+1)}\right]^2\left[\frac{\sigma - 2(\gamma+1)}{\sigma}\right]^2 , \tag{19}$$

and

$$x(\sigma) = x_1 + c_o(\sigma+1)(t_3-t_1)\left[\frac{\sigma_o}{\sigma_o - 2(\gamma+1)}\right]^2\left[\frac{\sigma - 2(\gamma+1)}{\sigma}\right]^2 , \tag{20}$$

TABLE I

Shock hydrodynamic data for aluminum. The first five columns are Los Alamos values for the pressure, p; the relative specific volume, V/V_o; the shock velocity, U; the particle velocity, u; and the sound velocity, c, behind the shock front. The values of pressure p and sound velocity c in the last two columns were computed from Fowles equation $p = 188.96\left[(V_o/V)^{4.266} - 1\right]$.

p Kilobar	$\frac{V}{V_o}$	U mm/μsec	u mm/μsec	c mm/μsec	p Kilobar	c mm/μsec
100	.9053	6.125	0.580	6.307	99.9	6.329
150	.8717	6.475	0.831	6.667	150.5	6.732
200	.8444	6.793	1.057	6.970	199.9	7.092
250	.8211	7.082	1.267	7.233	249.2	7.423
300	.8007	7.350	1.465	7.465	298.7	7.734
350	.7823	7.598	1.654	7.675	349.6	8.034
400	.7662	7.836	1.832	7.862	399.5	8.310
450	.7516	8.062	2.003	8.032	449.9	8.576
500	.7379	8.276	2.169	8.190	502.1	8.838
550	.7255	8.480	2.328	8.289	554.0	9.086
600	.7143	8.683	2.481	8.447	604.9	9.321
650	.7041	8.881	2.628	8.600	655.2	9.542
700	.6947	9.073	2.770	8.743	705.0	9.753
750	.6859	9.259	2.908	8.881	754.7	9.958
800	.6779	9.443	3.042	9.015	803.2	10.150
850	.6701	9.617	3.173	9.144	853.5	10.344
900	.6630	9.793	3.300	9.271	902.0	10.526
950	.6563	9.962	3.424	9.391	950.2	10.702
1000	.6498	10.126	3.546	9.508	999.6	10.877

where $$\sigma = (u + c - c_o)/c_o$$

and

$$\sigma_o = \frac{x_3 - x_1}{c_o(t_3 - t_1)} - 1 . \qquad (21)$$

The expressions for x_1, x_3, t_1 and t_3 are the same as those derived in the previous section.

Shock trajectories were calculated for initial conditions corresponding to the impact experiments discussed in the next section. In one set of calculations the Los Alamos shock wave data for aluminum were used to evaluate by numerical methods the integral appearing in Equations (14) and (15). A reproduction of the Los Alamos data is presented in the first five columns of Table I.

In the second set of calculations, the shock trajectories were obtained from Fowles' analytical solution using the same impact and particle velocities as those used for the first set of calculations. The density behind the shock front was obtained from Equation (18) and the initial shock velocity then calculated from the R-H equation for momentum. Values of x_1, t_1, x_3, and t_3 were obtained from Equations (5), (6), (9), and (10) using values of c_1 obtained from Equation (17). The shock trajectory was then calculated from Equations (19) and (20) using the value of σ_o obtained from Equation (21).

EXPERIMENTAL OBSERVATIONS

Precise data concerning the propagation of a shock can be obtained from optical records showing the emergence of the shock from the slant surface of a wedge, where the wedge angle is chosen sufficiently small to insure that the rarefaction from the slant surface does not enter behind the incident shock and alter its velocity. Commercially pure aluminum (1100F) was chosen for the present experiments. In an effort to minimize elastic-plastic effects associated with the finite yield strength of real metals[6], the aluminum was annealed by heating it to 750-800°F, holding for 2 hours, and then cooling at 50°F/hour to 500°F.

The wedge had an angle of 45 degrees and a square base whose sides were 5-1/4 inches. The striker plate was mounted on a 7-1/2 inch diameter charge and positioned 3/4 inch from the base of the wedge. The base charge was initiated by a 6 inch diameter planewave lens. Because of difficulty in maintaining the integrity of explosively accelerated plates, the strikers were made from 2024-T3 aluminum alloy. However, errors due to an elastic-plastic effect in the striker should be negligible when the shock trajectory is measured over a distance corresponding to more than twenty thicknesses of the striker. A diagram illustrating the essential features of the experimental arrangement is presented in Figure 2.

The explosive charge assemblies were varied to provide the three combinations of striker velocities and thicknesses shown in the table below:

Striker Thickness	Velocity
1/16 in. (1.588 mm)	5.800 mm/μsec
3/32 in. (2.381 mm)	5.130 mm/μsec
1/8 in. (3.175 mm)	4.136 mm/μsec

Two successful firings were obtained with 3/32 inch and 1/8 inch strikers. Only one successful firing was obtained with 1/16 inch strikers due to a malfunction of the initiation system.

The most accurate determination of impact velocity was obtained by using the linear part of the shock trajectory (that portion between $x = 0$ and $x = x_3$) to determine the initial shock velocities. The Hugoniot data for aluminum were then used to establish the corresponding values of u_1, which, in accordance with Equation (1), are one-half the impact velocities. The complete shock trajectory for the impact by the 3/32 inch plate is presented in Figure 3. Reproducibility of the shock trajectory is illustrated in Figure 3 by the excellent agreement between data obtained from two separate impacts.

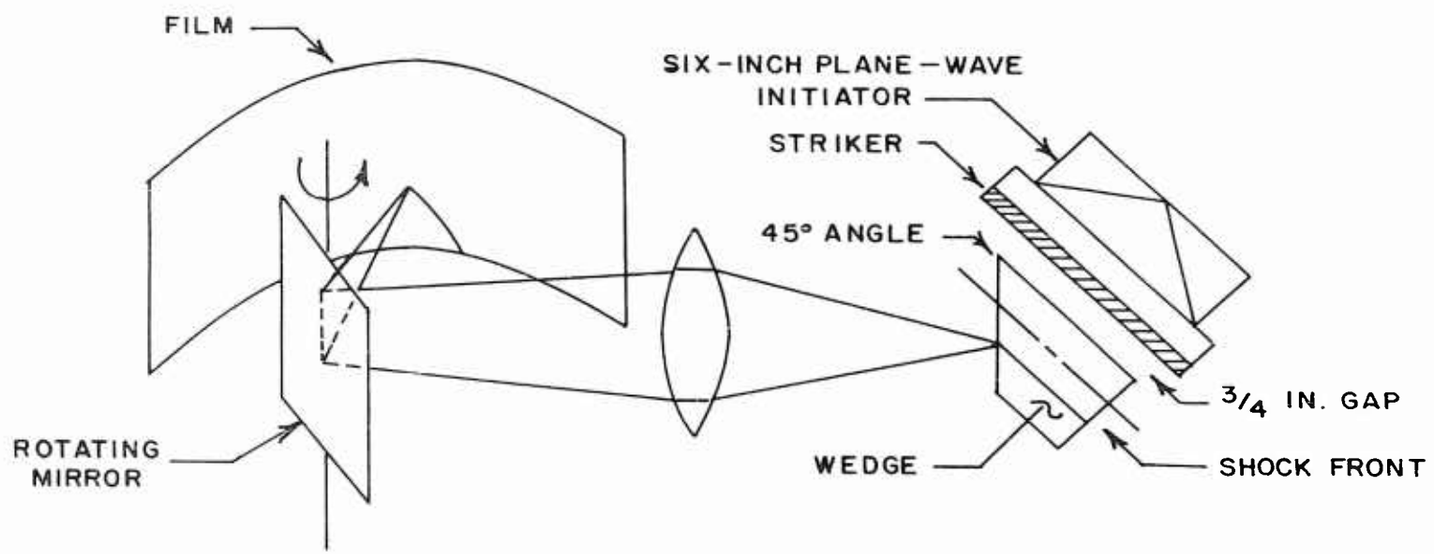

FIGURE 2. DIAGRAM ILLUSTRATING THE USE OF A ROTATING-MIRROR CAMERA TO MEASURE SHOCK ATTENUATION IN A METAL WEDGE.

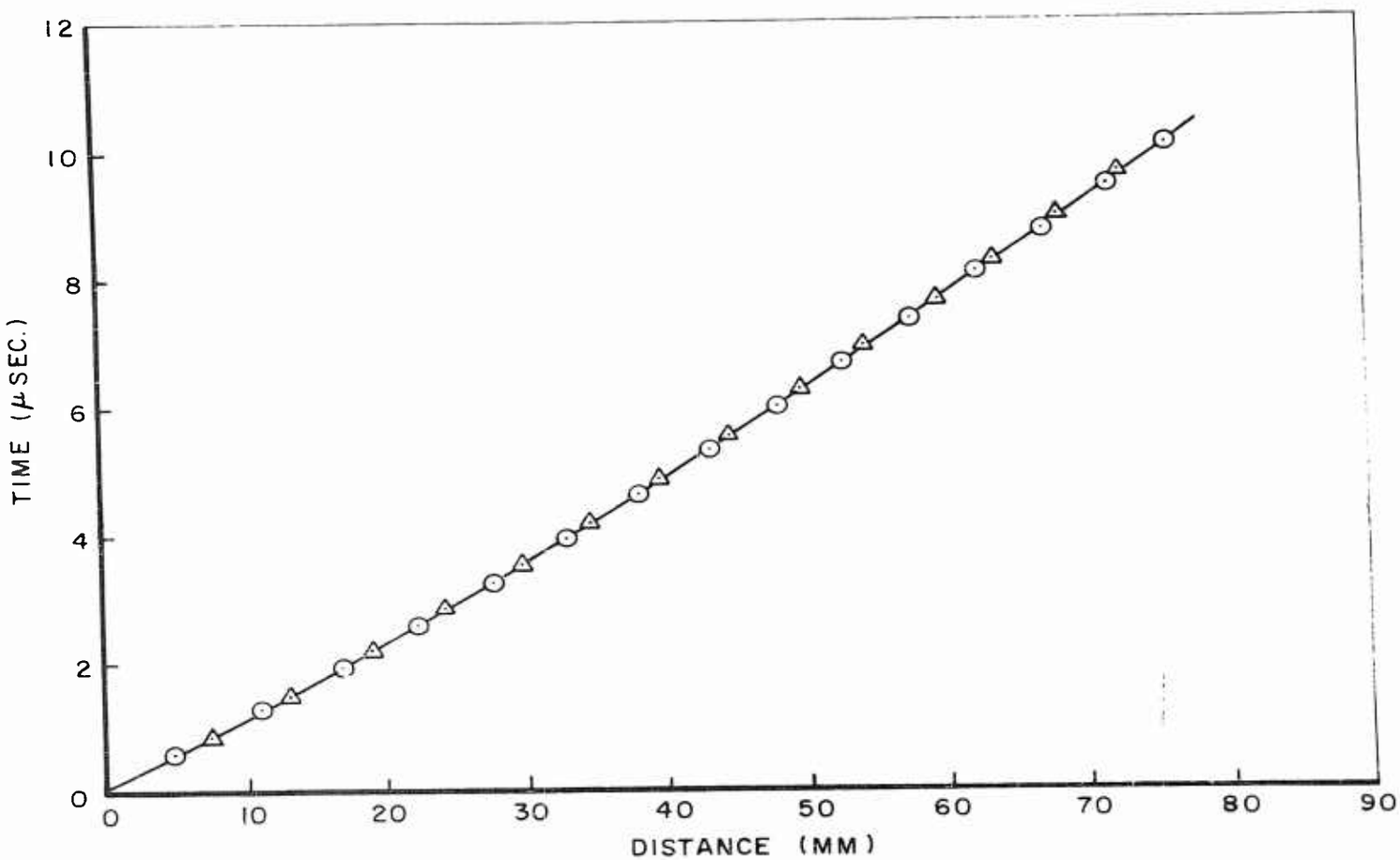

FIGURE 3- GRAPH SHOWING THE SHOCK TRAJECTORY RESULTING FROM A 3/32 IN. STRIKER IMPACTING AT 5.130 MM/μSEC. DATA FROM TWO SEPARATE IMPACTS ARE DISTINGUISHED BY USING CIRCLES FOR ONE AND TRIANGLES FOR THE OTHER.

DISCUSSION OF RESULTS

Arrival times for the shock at various depths in the target are presented in Table II. Column A represents experimental data; values in Column B were obtained from the Los Alamos sound velocity data using the $(u + c)$ = constant approximation of Chou et. al.; and values in Column C were calculated from Fowles equations. Times calculated using the Los Alamos sound velocity data are in excellent agreement with the experimental results, the maximum discrepancy being only 0.08 μsec. Although the differences are exceedingly small, results obtained from Fowles' equation show that neglect of entropy changes produces a shock attenuation which is more rapid than that observed experimentally. As would be expected entropy changes become less important as the initial shock strength decreases.

ACKNOWLEDGEMENTS

The author wishes to express his gratitude to members of the Physics Research Section for firing the shots and to Mr. Richard Vitali for assistance in analyzing the streak camera records.

F. E. ALLISON

TABLE II

Comparison of measured shock trajectories with those computed using two different approximations. Column A contains values interpolated from the experimental data, Column B contains values of t computed from the Los Alamos sound velocity data using the method of Chou, et al., and Column C contains values of t computed from Fowles' approximation neglecting the change in entropy across the shock.

	1/16 in.			3/32 in.			1/8 in.		
x mm	A μsec	B μsec	C μsec	A μsec	B μsec	C μsec	A μsec	B μsec	C μsec
0	0			0			0		
5	0.55			0.57			0.59		
10	1.10	1.08	1.08	1.13	1.14	1.13	1.19	1.23	1.23
15	1.67			1.70			1.80		
20	2.29	2.27	2.31	2.30	2.29	2.31	2.44	2.45	2.45
25	2.93			2.92			3.09		
30	3.59	3.58	3.67	3.56	3.55	3.60	3.74	3.71	3.73
35	4.26			4.22			4.39		
40	4.95	4.97	5.09	4.90	4.88	4.96	5.05	5.03	5.09
45	5.65			5.59			5.73		
50	6.36	6.41	6.56	6.28	6.27	6.39	6.41	6.42	6.50
55	7.08			6.98			7.11		
60	7.81	7.89	8.07	7.68	7.70	7.84	7.84	7.84	7.94
65	8.56			8.38			8.57		
70	9.32			9.16	9.17	9.33	9.33	9.30	9.42
75	10.09			9.97			10.12		

REFERENCES

1. Fowles, G. R. Attenuation of the Shock Wave Produced in a Solid by a Flying Plate. J. Appl. Phys., Vol. 31, No. 4, pp 655-661, April 1960.

2. Chou, Pei Chi, Sidhu, Harbans S., and Zajac, Lawrence J. Attenuation of the Strong Plane Shock Produced in a Solid by Hypervelocity Impact. Drexel Institute of Technology Report No. 125-5, Contract No. DA-36-034-ORD-3672 RD, February 1964.

3. Al'tshuler, L. V., Kormer, S. B., Brazhnik, M. I., Vladimirov, L. A., Speranskaya, M. P., and Funtikov, A. I. The Isentropic Compressibility of Aluminum, Copper, Lead, and Iron at High Pressures. Soviet Physics JETP, Vol. II, No. 4, October 1960.

4. Murnaghan, D. F. Finite Deformation of an Elastic Solid. John Wiley and Sons, Inc., New York (1951).

5. Rice, M. H., McQueen, R. G., and Walsh, J. M. Compression of Solids by Strong Shock Waves. Solid State Physics, Vol. 6, Edited by Frederick Seitz and David Turnbull, Academic Press, Inc., New York and London (1958).

6. Fowles, G. R. Shock Wave Compression of Hardened and Annealed 2024 Aluminum. J. Appl. Physics, Vol. 32, No. 8, pp 1475-1487, August 1961.

DISTRIBUTION LIST

No. of Copies	Organization
20	Commander Defense Documentation Center ATTN: TIPCR Cameron Station Alexandria, Virginia 22314
2	Chief, Defense Atomic Support Agency Washington, D. C. 20301 Of Interest to: Major B. M. Carswell Blast and Shock Section
1	Director of Defense Research and Engineering (OSD) The Pentagon Washington, D. C. 20301
1	Commanding General U. S. Army Materiel Command ATTN: AMCRD-RP-B Washington, D. C. 20315
1	Commanding Officer Picatinny Arsenal ATTN: Mr. J. Hershkowitz Dover, New Jersey 07801
1	Commanding Officer Harry Diamond Laboratories Washington, D. C. 20438
1	Commanding General U. S. Army Engineering Research and Development Lab ATTN: STINFO Branch Fort Belvoir, Virginia 22060
1	Colorado School of Mines ATTN: Dr. John Rinehart Golden, Colorado

No. of Copies	Organization
1	Army Research Office 3045 Columbia Pike Arlington, Virginia 22204
1	Commanding Officer U. S. Army Research Office (Durham) ATTN: CRD-AA-IPL Box CM, Duke Station Durham, North Carolina 27706
1	Chief of Research and Development ATTN: Army Research Office Department of the Army Washington, D. C. 20310
3	Chief, Bureau of Naval Weapons ATTN: DLI-3 Department of the Navy Washington, D. C. 20360
1	Commander U. S. Naval Ordnance Test Station China Lake, California 93557
2	Commander U. S. Naval Ordnance Laboratory White Oak Silver Spring, Maryland 20910
1	Director U. S. Naval Research Laboratory Washington, D. C. 20390
1	AFWL (WLL) Kirtland AFB New Mexico 87117
1	AFML (MAY) Wright-Patterson AFB Ohio

DISTRIBUTION LIST

No. of Copies	Organization
1	Library of Congress Technical Information Division ATTN: Bibliography Section Reference Department Washington 25, D. C.
1	U. S. Department of Interior Bureau of Mines ATTN: Chief, Explosive and Physical Sciences Div. 4800 Forbes Street Pittsburgh, Pennsylvania 15213
2	U. S. Atomic Energy Commission Los Alamos Scientific Lab P. O. Box 1663 Los Alamos, New Mexico 87544
1	U. S. Atomic Energy Commission ATTN: Technical Reports Library Washington, D. C. 20545
2	U. S. Atomic Energy Commission Lawrence Radiation Laboratory P. O. Box 808 Livermore, California 94550
1	Professor Pei Chi Chou Drexel Institute of Technology 32nd and Chestnut Streets Philadelphia 4, Pennsylvania
1	Professor N. Davids Pennsylvania State University University Park, Pa. 16802
1	Professor E. H. Lee Leland Stanford Junior University Davidson of Engineering Mechanics Stanford, California
1	Dr. G. R. Fowles Stanford Research Institute Poulter Laboratories Menlo Park, California
1	Dr. S. J. Lukasik Stevens Institute of Technology Davidson Laboratory Hoboken, New Jersey
1	Brown University Division of Engineering Providence, Rhode Island
1	Batelle Memorial Institute 505 King Street Columbus, Ohio 43201
1	General Dynamics Corporation General Atomic Division ATTN: Dr. J. M. Walsh P. O. Box 608 San Diego, California
1	The General Electric Company Missiles and Space Division ATTN: Dr. T. Rinig 3198 Chestnut Street Philadelphia 4, Pennsylvania
1	General Motors Corporation Defense Systems Division Box T Santa Barbara, California 93100
1	Minneapolis-Honeywell Regulator Company Ordnance Division ATTN: Donald M. Catton 600 2nd Street, North Hopkins, Minnesota

DISTRIBUTION LIST

No. of Copies	Organization
4	Australian Group c/o Military Attache Australian Embassy 2001 Connecticut Avenue, N. W. Washington, D. C. 20008
10	The Scientific Information Officer Defence ~~Research~~ Staff British Embassy 3100 Massachusetts Avenue, N. W. Washington, D. C. 20008
4	Defence Research Member Canadian Joint Staff 2450 Massachusetts Avenue, N. W. Washington, D. C. 20008
	Aberdeen Proving Ground
	Chief, TIB
	Air Force Liaison Office Marine Corps Liaison Office Navy Liaison Office CDC Liaison Office
	D & PS Branch Library

Unclassified
Security Classification

DOCUMENT CONTROL-DATA - R&D

(Security classification of title, body of abstract and indexing annotation must be entered when the overall report is classified)

1 ORIGINATING ACTIVITY *(Corporate author)* Ballistic Research Laboratories Aberdeen Proving Ground, Maryland	2a REPORT SECURITY CLASSIFICATION Unclassified 2b GROUP

3 REPORT TITLE

ATTENUATION OF PLANE SHOCK FRONTS IN ALUMINUM

4 DESCRIPTIVE NOTES *(Type of report and inclusive dates)*

5 AUTHOR(S) *(Last name, first name, initial)*

Allison, Floyd E.

6. REPORT DATE	7a. TOTAL NO. OF PAGES	7b. NO. OF REFS
November 1964	27	6

8a. CONTRACT OR GRANT NO. b. PROJECT NO. 1M010501A009 c. d.	9a. ORIGINATOR'S REPORT NUMBER(S) Memorandum Report No. 1606 9b. OTHER REPORT NO(S) *(Any other numbers that may be assigned this report)*

10. AVAILABILITY/LIMITATION NOTICES

Qualified requesters may obtain copies of this report from DDC.

11. SUPPLEMENTARY NOTES	12 SPONSORING MILITARY ACTIVITY
	Work was partially supported by the Advanced Research Projects Agency

13 ABSTRACT

The attenuation of a plane shock wave by an overtaking rarefaction has been studied using a rotating-mirror streak camera to obtain a shock trajectory resulting from the impact of a thin striker. Experimental data are presented for shocks in 1100F aluminum and tha data are compared with results obtained from two sets of calculations. The shock attenuation is in excellent agreement with calculations based on linear characteristics along which (u + c) is constant. The attenuation is measurably less than that calculated from Fowles' equations, which neglect entropy changes at the shock front.

DD FORM 1 JAN 64 1473

Unclassified
Security Classification

14 KEY WORDS	LINK A		LINK B		LINK C	
	ROLE	WT	ROLE	WT	ROLE	WT
Shock Hydrodynamics Theory of Attenuation Shock Attenuation (Aluminum) Rarefaction Waves						

INSTRUCTIONS

1. ORIGINATING ACTIVITY: Enter the name and address of the contractor, subcontractor, grantee, Department of Defense activity or other organization *(corporate author)* issuing the report.

2a. REPORT SECURITY CLASSIFICATION: Enter the overall security classification of the report. Indicate whether "Restricted Data" is included. Marking is to be in accordance with appropriate security regulations.

2b. GROUP: Automatic downgrading is specified in DoD Directive 5200.10 and Armed Forces Industrial Manual. Enter the group number. Also, when applicable, show that optional markings have been used for Group 3 and Group 4 as authorized.

3. REPORT TITLE: Enter the complete report title in all capital letters. Titles in all cases should be unclassified. If a meaningful title cannot be selected without classification, show title classification in all capitals in parenthesis immediately following the title.

4. DESCRIPTIVE NOTES: If appropriate, enter the type of report, e.g., interim, progress, summary, annual, or final. Give the inclusive dates when a specific reporting period is covered.

5. AUTHOR(S): Enter the name(s) of author(s) as shown on or in the report. Enter last name, first name, middle initial. If military, show rank and branch of service. The name of the principal author is an absolute minimum requirement.

6. REPORT DATE: Enter the date of the report as day, month, year; or month, year. If more than one date appears on the report, use date of publication.

7a. TOTAL NUMBER OF PAGES: The total page count should follow normal pagination procedures, i.e., enter the number of pages containing information.

7b. NUMBER OF REFERENCES: Enter the total number of references cited in the report.

8a. CONTRACT OR GRANT NUMBER: If appropriate, enter the applicable number of the contract or grant under which the report was written.

8b, &c, & 8d. PROJECT NUMBER: Enter the appropriate military department identification, such as project number, subproject number, system numbers, task number, etc.

9a. ORIGINATOR'S REPORT NUMBER(S): Enter the official report number by which the document will be identified and controlled by the originating activity. This number must be unique to this report.

9b. OTHER REPORT NUMBER(S): If the report has been assigned any other report numbers *(either by the originator or by the sponsor)*, also enter this number(s).

10. AVAILABILITY/LIMITATION NOTICES: Enter any limitations on further dissemination of the report, other than those imposed by security classification, using standard statements such as:

(1) "Qualified requesters may obtain copies of this report from DDC."

(2) "Foreign announcement and dissemination of this report by DDC is not authorized."

(3) "U. S. Government agencies may obtain copies of this report directly from DDC. Other qualified DDC users shall request through _____."

(4) "U. S. military agencies may obtain copies of this report directly from DDC. Other qualified users shall request through _____."

(5) "All distribution of this report is controlled. Qualified DDC users shall request through _____."

If the report has been furnished to the Office of Technical Services, Department of Commerce, for sale to the public, indicate this fact and enter the price, if known.

11. SUPPLEMENTARY NOTES: Use for additional explanatory notes.

12. SPONSORING MILITARY ACTIVITY: Enter the name of the departmental project office or laboratory sponsoring *(paying for)* the research and development. Include address.

13. ABSTRACT: Enter an abstract giving a brief and factual summary of the document indicative of the report, even though it may also appear elsewhere in the body of the technical report. If additional space is required, a continuation sheet shall be attached.

It is highly desirable that the abstract of classified reports be unclassified. Each paragraph of the abstract shall end with an indication of the military security classification of the information in the paragraph, represented as *(TS)*, *(S)*, *(C)*, or *(U)*.

There is no limitation on the length of the abstract. However, the suggested length is from 150 to 225 words.

14. KEY WORDS: Key words are technically meaningful terms or short phrases that characterize a report and may be used as index entries for cataloging the report. Key words must be selected so that no security classification is required. Identifiers, such as equipment model designation, trade name, military project code name, geographic location, may be used as key words but will be followed by an indication of technical context. The assignment of links, rules, and weights is optional.